POAC'15
Trondheim, Norway

Proceedings of the 23rd International Conference on
Port and Ocean Engineering under Arctic Conditions
June 14-18, 2015
Trondheim, Norway

NEAR SEA ICE, OCEAN CURRENT AND TURBULENCE MEASURMENTS IN THE CHUKCHI SEA

Todd Mudge[1], Robert Raye[2], Keath Borg[1], Nikola Milutinovic[1], Dawn Sadowy[1], David B. Fissel[1] and Ed Ross[1]
[1]ASL Environmental Sciences Inc, Victoria, Canada
[2] Shell Exploration and Production, Anchorage, USA

ABSTRACT

Measurements of ocean currents, sea ice motion and ice draft have been made using upward looking sonar (ULS) datasets since 2008 for Shell in the Chukchi Sea. An Acoustic Doppler Current Profiler (ADCP) typically provides one to several minutes temporal resolution for currents and ice velocity and a 1 to 2 m vertical resolution for currents. An Ice Profiling Sonar (IPS) provides vertical resolution of better than 0.05 m for ice drafts and a temporal resolution of 1-2 seconds.

Near ice boundary layer currents measurements are critical to understand the interaction between sea ice and the underlying ocean. These measurements allow for a better understanding of processes such as heat flux and ocean tracer mixing and thus they provide insight into the melting of sea ice from below and dispersion of oil and oil dispersants. Sea ice in the Chukchi Sea has a high degree of deformation, upwards of tens of metres, making the measurements of the near sea ice boundary currents challenging. ASL has developed semi-automated algorithms that accounts for the changing ice-canopy in order to measure these currents.

Further algorithm development allows for the analysis of all valid current bins from the ADCP. By combining this analysis with ASL's standard ice velocity analysis, currents can be put into an ice-centric frame. These currents can be fitted to a law-of-the-wall logarithmic curve and thus ice roughness and turbulence parameters can be derived. Previous analysis has been completed for one of Shell's sites from the 2012-13 ice season (Mudge et al. 2014). Additional data sets and improved procedures allow for the modelling of drag coefficient from IPS derived roughness.

Introduction

Sea Ice

The boundary layer dynamics of ocean and sea ice interaction are challenging to study. The impacts on currents, turbulence and drag of the varied sea ice conditions, from level ice of a few metres thick to keels with thicknesses of tens of metres and rubbled ice with horizontal extents of many hundreds of metres need to be understood. There have been various current measurement programs deployed from the ice (McPhee 2013; Mudge 2005); unfortunately, they are preferentially measured where there is level ice due to the logistical difficulty in deploying through highly deformed ice features. They are of a short extent and must drift with the ice; thus limiting their usefulness in understanding ice/ocean dynamics over a long period of time at an individual location.

Ocean current and ice draft measurements have been made for over a decade, often with multiyear deployments in various seas around the Arctic, by using Upward Looking Sonars (ULS) by research groups, such as Department of Fisheries and Oceans Canada (DFO), ArcticNet, Woods Hole Oceanographic Institute and Norwegian Polar Institute, and for oil and gas companies. These subsurface deployments need to be below the deepest ice keels, making near ice measurements within the first few metres of the ice/ocean boundary layer impossible where ice is highly deformed. Recent developments in processing algorithms at ASL has extended valid current measurements throughout the water column and as near to the ice as possible. This has allowed for the measurement of the turbulent boundary layer under specific conditions.

Deployments near Alaska

Since 2008, ASL has supported Shell's sea ice draft, ice drift and ocean currents measuring program in the Chukchi Sea (Figure 1). A concurrent program had been running in the Beaufort Sea's Camden Bay region from 2005 to 2013 and Harrison Bay region from 2012 to 2014. These measurement programs included collaborations with Dr. Humfrey Melling of DFO until 2008 when Olgoonik-Fairweather became the prime contractor for the projects. Most of the measurements have been made from taut-line mooring pairs: a Teledyne RDI Acoustic Doppler Current Profiler (ADCP) in one and an ASL Ice Profiling Sonar (IPS) in the second, placed about 100 m apart (Figure 2). Metocean inputs for engineering design and operational planning has been the primary driver for the programs.

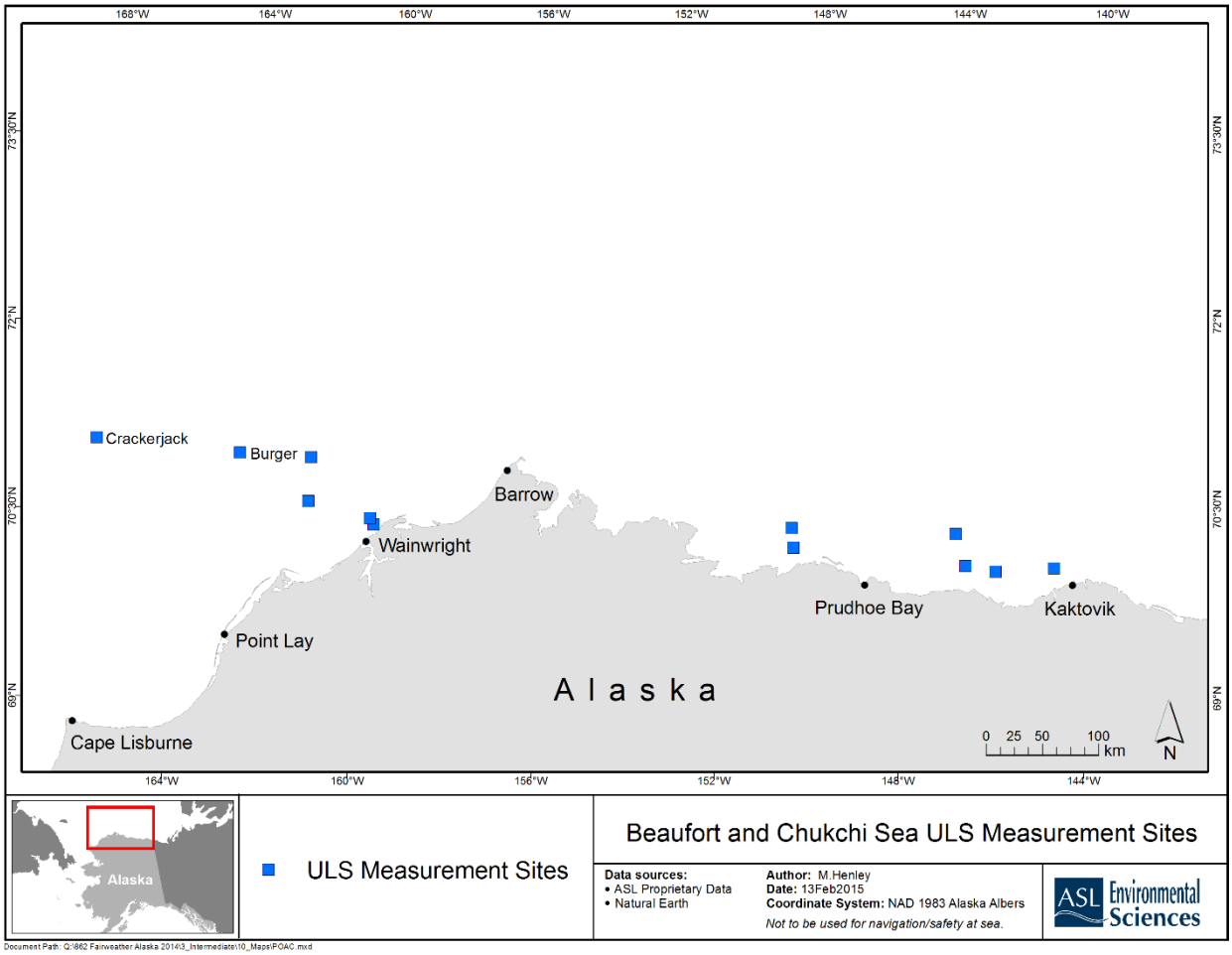

Figure 1. Shell's Upward Looking Sonar sites in the Chukchi and Beaufort Seas. Analysis of data acquired at Crackerjack and Burger was used to derive turbulence parameters.

Upward Looking Sonars

Acoustic Doppler Profilers

Shell's sites in the Chukchi and Beaufort Sea have been instrumented with Sentinel Workhorse ADCPs, manufactured by Teledyne RD Instruments of Poway, California. The Sentinel ADCPs were modified by RDI in 1996 to use the Doppler shift from the ice bottom surface to measure ice velocity, and backscatter on each beam to determine the distances to the ice. Velocities are measured by four acoustic beams oriented 20 degrees off vertical which detect the Doppler shift in acoustic frequency arising from water current (or ice) movements. The ADCPs were configured to measure ocean currents with a vertical resolution (bin size) of 2 m at 5 minute sample rates.

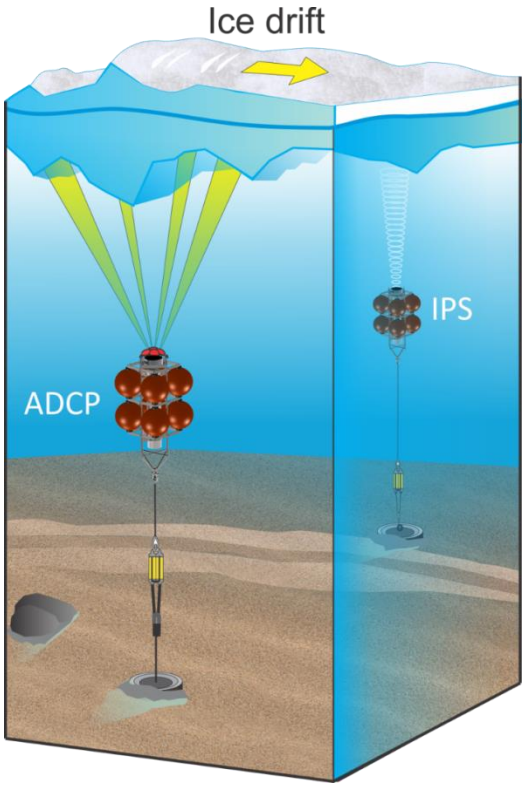

Figure 2. Acoustic Doppler Current Profiler (left) and Ice Profiling Sonar (right) taut line moorings as deployed in the Chukchi and Beaufort Seas.

Ice Profiling Sonars

The IPS instrument is an upward-looking ice profiling sonar that measures ice draft. This instrument was originally designed by the Institute of Ocean Sciences, DFO (Melling et al., 1995), and has been further developed and subsequently manufactured by ASL. The ice keel depth is determined from the return travel time of an acoustic pulse (420 kHz; 1.8° beam at -3 dB) reflected off the underside of the sea ice. The return time is converted to an acoustic range value through the use of the speed of sound in seawater.

In the Chukchi and Beaufort Seas programs, the current version of ASL's ice profiler (IPS5; Fissel et al., 2007), was setup to run through various configurations (phases) to acquire the highest temporal resolution data based on climatological conditions. Ice phases sampled continuously every 1 or 2 seconds providing better than 1 m horizontal resolution of ice draft during the winter. During shoulder months, 1 Hz sampling provided both continuous ice draft and waves measurements, depending upon ice coverage. During the summer months, 2 Hz wave bursts provided non-directional wave data.

Turbulence Theory

Classic law-of-the-wall (Tennekes and Lumley, 1972) turbulent boundary layers have been measured within the near-ice boundary layer (McPhee 2013), but there have been more studies of the near-bottom boundary layer (Lueck and Lu, 1997). Viscous stresses dominate within the first few centimetres of an oceanographic boundary layer (Figure 3). Beyond the viscous and transitional buffer layers, turbulence stresses dominate and the mean current follows,

$$U = \frac{u_*}{\kappa} \cdot \ln\left(\frac{z_r}{z_o}\right) \quad (1)$$

where u_* is the friction velocity, κ is the von Kármán's constant (~0.4) and z_o is the roughness length. From bottom boundary studies, the roughness length scales at about one thirtieth of the sand grain diameter. The drag coefficient can be determined for a reference height z_r as

$$c_d = \frac{\kappa}{\ln\left(\frac{z_r}{z_o}\right)^2} \quad (2)$$

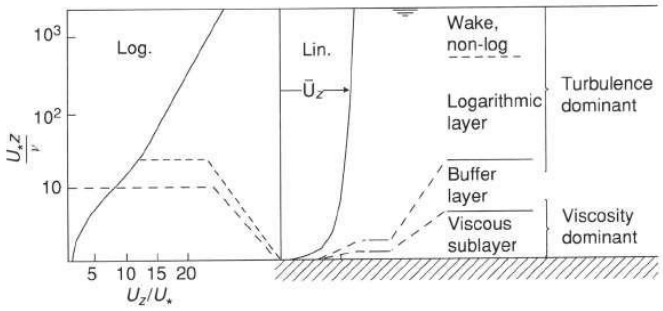

Figure 3. Law-of-the-wall boundary layer structure. The vertical axis is logarithmic (Log.) and linear (Lin.) (McCave, 2005)

The development of a logarithmic layer requires strong and steady forcing, such as a steady current or ice drift. The presence of the logarithmic layer is impacted by the Coriolis force and the presence of the Ekman layer (Ekman 1905) and by the presence of density stratification. Thus we need to ensure that the turbulent boundary layer dominates the Coriolis force. This scales as a distance, $\kappa \bullet u_* / f$ from the boundary, where f is the Coriolis frequency. Perlin at al. (2005) showed that stratification supports a greater velocity shear, resulting in an artificially large friction velocity. To apply Eq 1, directly to our data we must ensure that the stratification is small and we remove any examples where we derive artificially large friction velocities. The relatively shallow Chukchi Sea is an ideal area to work, as buoyancy driven mixing due to heat loss and the extrusion of salt brine associated with the formation of sea ice effectively mixes the underlying water column to the ocean bottom. In the spring or early summer, stratification is likely to occur due to sea ice melt and advection of warm Pacific waters.

Conditions to develop a logarithmic layer are most easily achieved within a few metres of the ice/ocean interface; thus most studies have been done by hanging instruments from the ice. To develop a logarithmic layer that can be detected by the ADCPs in the Chukchi Sea, taut-line moorings require ice velocities that are both large and steady when stratification is low.

Limiting ourselves to these conditions, there are likely around 100 potential cases to study within the 14 site-years of data from the Chukchi Sea sites.

Analysis Methods

The ADCP measures currents through the water column; however, making measurements near the ice/water interface is non-trivial. The ice/water interface is a complex surface which changes with time (Figure 4). The ADCP's Janus configuration requires at least three Doppler returns of the four transducers to be from the water and not contaminated by the presence of ice. The closest measurable current is additionally limited by "side-lobe" interference, where strong acoustic returns from the ice, usually along a direct vertical path, contaminate weaker backscatter returns coming from the water that travel along the centre of the acoustic beam which is slanted 20º off vertical. For flat ice, the region of side-lobe interference is the first 6 % of the ADCP current profile.

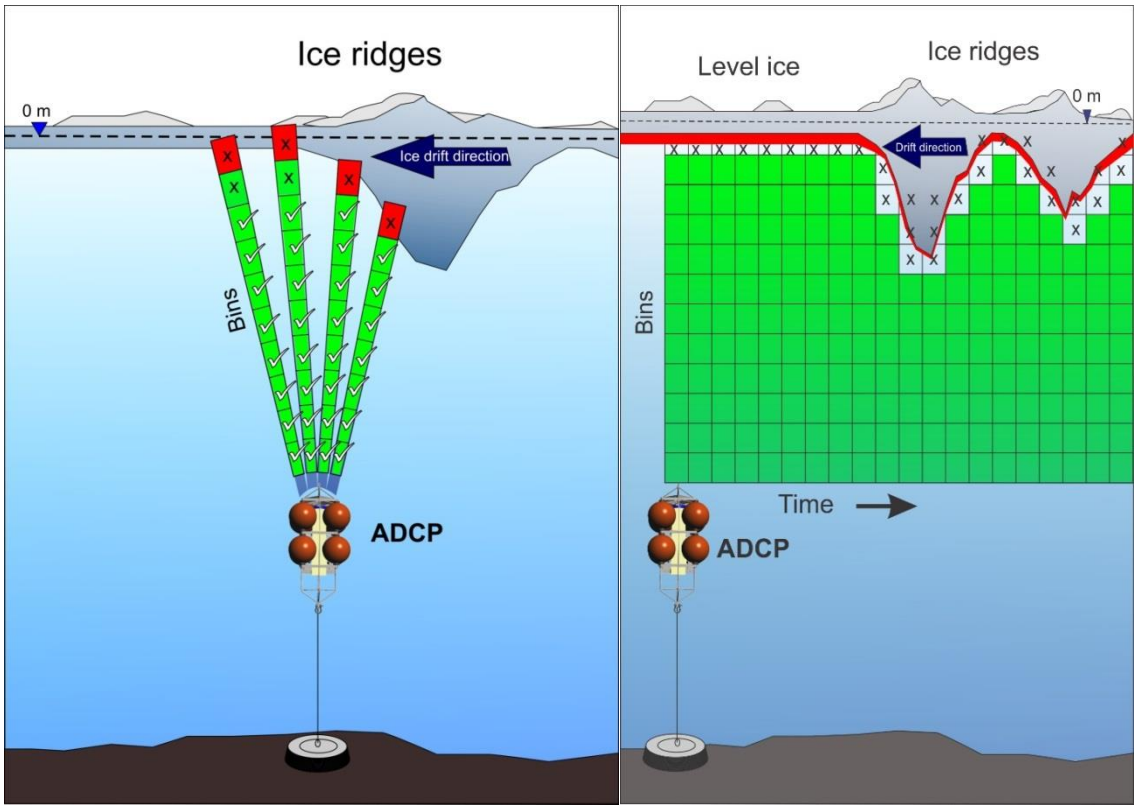

Figure 4. On the left, the ADCP's four acoustic beams with valid Doppler solutions (green) and valid three or four beam solutions (check marks). On the right, ADCP bins with valid Doppler solutions (green) and partially obscured bins (marked by X) as ice keels drift past. Red depicts the region (approximately 6% of the distance from the ADCP to the ice) where Doppler returns from the water column are contaminated by returns from the ice.

Teledyne RDI ADCPs use separate acoustic pings to measure water currents and bottom track velocities, which in the presence of ice is the ice drift velocity. Both the currents and ice drift are automatically corrected for changes in sound speed. The sound speed is calculated from ADCP measured temperature and a user input salinity, 32 PSU for the Chukchi Sea. Bottom track ranges, distances to the ice, are also corrected for sound speed changes. Current bins, 2 m for the Chukchi data, are kept the same size by using a constant sound speed of 1500 m/s. The mismatch in sound speeds for the bottom track ranges and the bins would create errors in

the boundary analysis. To reduce these, the bottom track ranges were scaled to a constant sound speed of 1500 m/s.

The bottom track ranges from the ADCP were used to determine the shallowest valid current bins (Figure 5). For each ensemble (5 minutes for the Chukchi data), the ADCP measures a bottom track range for each of the four beams. A semi-automatic algorithm uses the third shallowest range to determine where the shallowest valid currents are detectable. The median of the bottom track ranges during a turbulence event of interest is nominally considered "level ice", and we reference all of our vertical distances from this level.

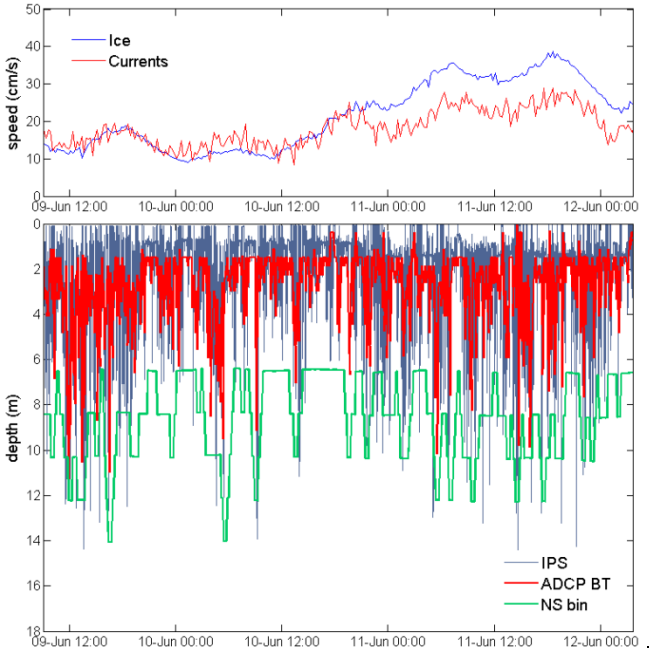

Figure 5. Example section of near surface bin current speed and ice drift speed under a rough ice canopy (top panel). Ice draft as measured by IPS (blue), distance to ice as measured by the ADCP bottom track (red) and resultant near surface bin depth (green) (bottom panel) (Mudge et al. 2014).

To analyze the turbulent boundary layer, the ocean current data was converted from an earth reference frame into an ice reference frame. The measured ice drift was subtracted from the measured currents at each depth (Figure 6).

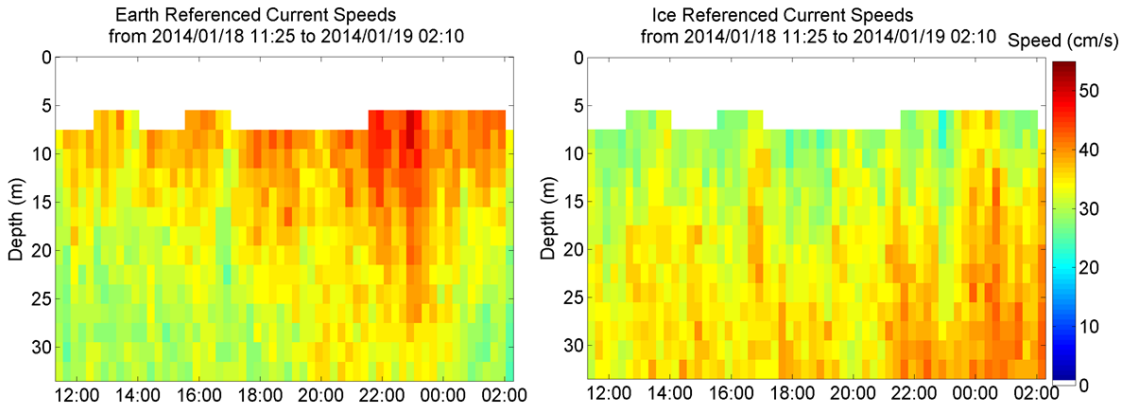

Figure 6. Currents relative to the fixed earth reference frame (left) are converted to an ice based reference frame (right).

The conditions to develop a detectable logarithmic layer with a taut-line moored ADCP in the Chukchi Sea only exists for a few days each year. However, the IPS provides continuous high spatial resolution ice draft throughout the entire ice season. By comparing ADCP derived roughness, z_o, to IPS derived ice roughness, an empirical model can be developed that will allow for the estimation of, z_o, and drag coefficients for times and locations where no logarithmic layer could be detected by a taut-line ADCP. The IPS derived roughness, σ_{IPS}, is based on the standard deviation of a high passed ice-draft spatial series. Long wavelength variability in the ice canopy, which would not induce turbulence, was removed by using a fifth order Butterworth high pass filter with a 300 m cut-off wavelength.

Small and Large Roughness Scale Examples

On November 27, 2012, there was a large ice motion event at the Crackerjack site. The ice is mostly smooth during the event, as illustrated in the top left panel of Figure 7. The associated current profile in the ice reference frame is in the lower left panel. A second example from Burger on January 21, 2014, in the upper right hand panel of Figure 7, illustrates the ice is heavily deformed with several keels, some with nearly 15 m drafts.

Figure 8 shows the vector average current speeds and a logarithmic curve as expected from the law of the wall. Only points illustrated with circles have been included in the logarithmic fit. For the smooth ice case, the fitted curve can be used to derive a roughness length, $z_{o,}$ of 0.58 cm, and a friction velocity, u_*, of 2.5 cm/s. The associated roughness in the ice drafts, σ_{IPS}, is 39.8 cm. For the rough ice case, the fitted curve produces a z_o of 12.1 cm, and a friction velocity, u_*, of 2.5 cm/s. Ice roughness, $\sigma_{IPS,}$ was 150.7 cm during this event, or about 12 times larger than the bottom roughness.

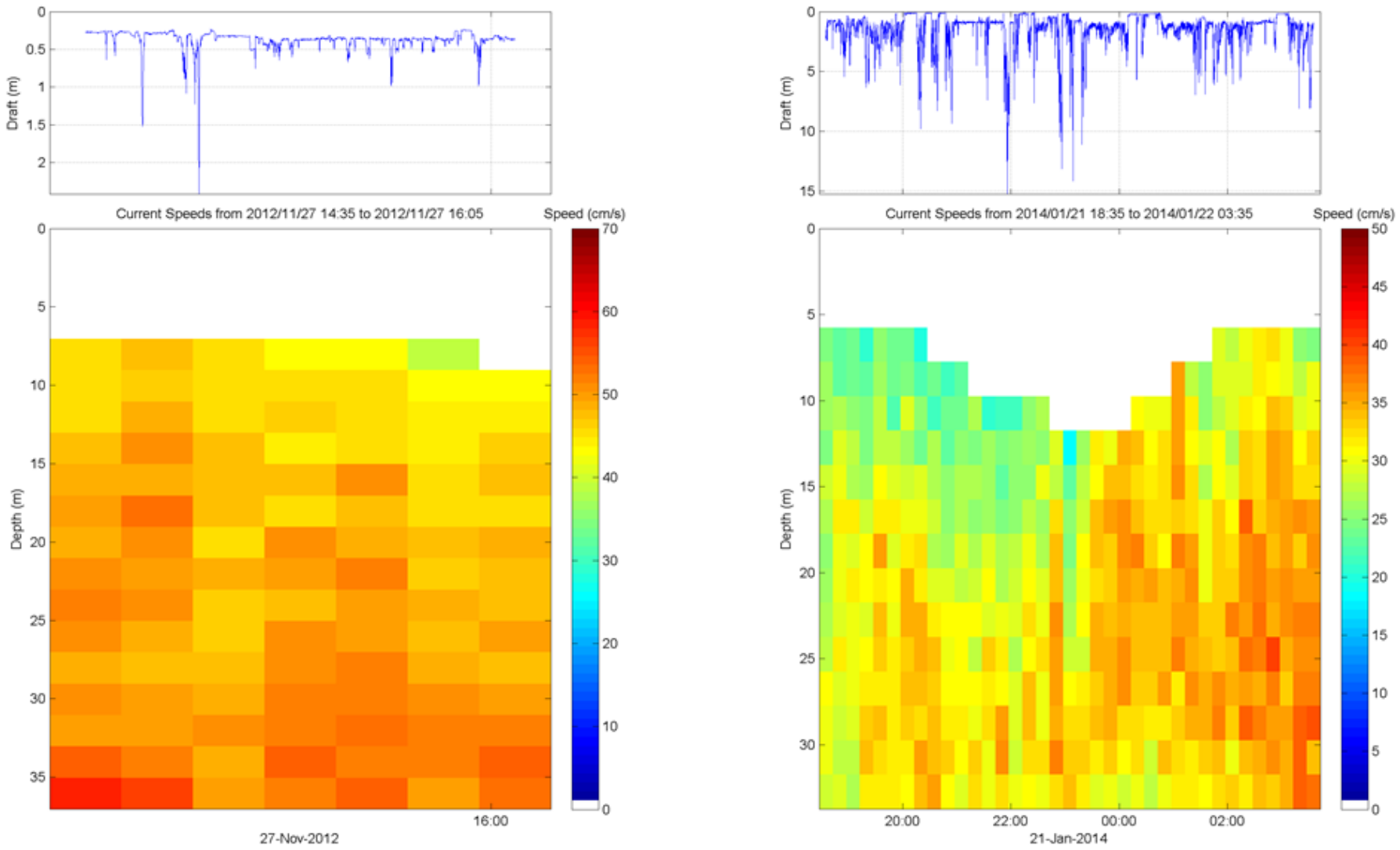

Figure 7. Ice draft (top panels) and current profiles (bottom panels) for a smooth ice case at Crackerjack (left) and a rough ice case at Burger (right).

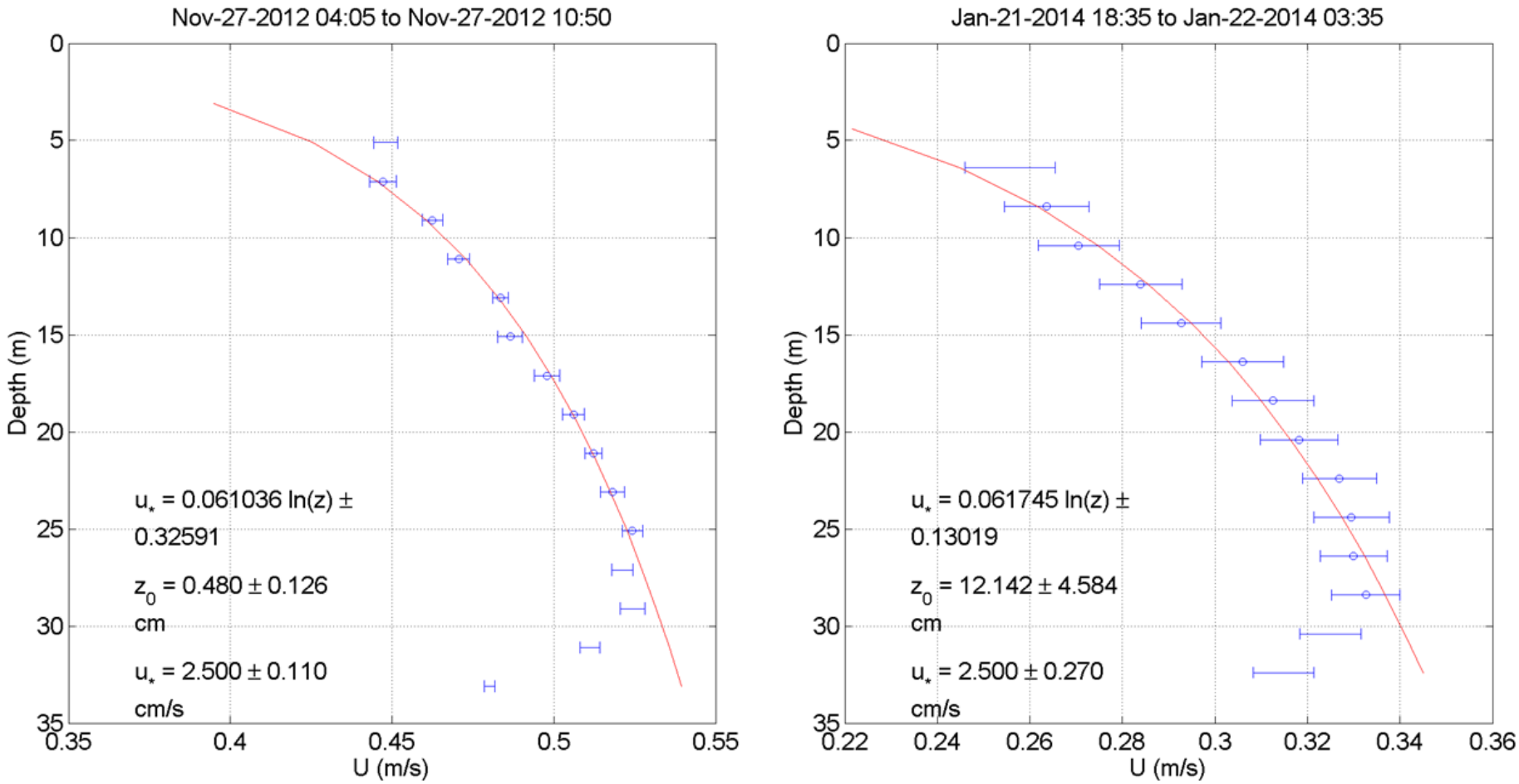

Figure 8. Current profile for a smooth ice case at Crackerjack (left) and a rough ice case for Burger (right). The red curve is the fitted law of the wall profile, based on the points illustrated with circles.

Summary of Turbulent Boundary Examples

There have been 18 events of high quality logarithmic layers detected, by using data from the Burger and Crackerjack sites during two ice seasons. Table 1 provides a summary of the ADCP derived turbulence properties and associated IPS derived ice roughness. The scale upon which the turbulent boundary layer dominates the Coriolis force is $\kappa \bullet u_* / f$, where f, the Coriolis frequency, is $f = 2\ 7.2921 \times 10^{-5}$ rad/s *sin(latitude)*. Taking the Chukchi Sea as 71°N, then turbulence dominates the Coriolis force in the upper 29 m when the friction velocity, u_*, is equal to 1 cm/s. The measured logarithmic boundary layer thicknesses, ranging from 19 to 33 m, are well within the region dominated by turbulence given the friction velocities range from 1.5 to 2.8 cm/s

Table 1. Summary of the site name (BU – Burger, CJ – Crackerjack), start and end date, roughness length scale z_o, friction velocity u_*, drag coefficient c_d for z_r = 1m, the vector average ice drift speed $\langle V_{ice} \rangle$, the depth of the logarithmic boundary layer and IPS derived roughness σ_{IPS}.

Site	Start	End	ADCP					IPS
			z_o (cm)	u_* cm/s	c_d	<Vice> (cm/s)	Bnd. Layer (m)	σ_{IPS} (m)
CJ	27 Nov 2012 04:05	27 Nov 2013 10:50	0.480	2.502	0.006	51.4	25	0.398
CJ	27 Nov 2012 14:35	27 Nov 2013 16:05	0.024	1.784	0.002	51.8	19	0.170
CJ	21 Dec 2012 10:35	21 Dec 2013 19:50	1.145	2.454	0.008	55.5	24	0.566
CJ	21 Dec 2012 16:20	21 Dec 2013 20:05	0.136	1.964	0.004	58.6	23	0.490
CJ	21 Dec 2012 20:05	22 Dec 2013 02:05	0.007	1.368	0.002	58.5	24	0.124
CJ	14 Jan 2013 11:04	14 Jan 2013 13:04	3.451	2.826	0.015	58.8	33	0.606
CJ	14 Jan 2013 13:19	14 Jan 2013 17:04	0.348	2.075	0.005	57.8	30	0.765
BU	23 Nov 2013 10:20	23 Nov 2013 13:20	2.817	2.836	0.013	73.7	23	0.213
BU	23 Nov 2013 13:20	23 Nov 2013 16:50	0.417	1.937	0.006	66.8	23	0.035
CJ	23 Nov 2013 13:55	23 Nov 2013 20:40	0.011	1.538	0.002	70.1	33	0.393
CJ	30 Nov 2013 10:40	30 Nov 2013 14:40	1.881	2.644	0.011	65.8	31	0.315
BU	01 Dec 2013 00:50	01 Dec 2013 06:05	0.341	2.534	0.005	74.7	31	0.552
BU	01 Dec 2013 06:05	01 Dec 2013 08:20	0.008	1.872	0.002	75.5	23	0.290
BU	21 Dec 2013 17:05	22 Dec 2013 04:20	3.194	2.155	0.014	53.8	33	0.519
BU	06 Jan 2014 20:05	07 Jan 2014 03:05	6.197	2.272	0.022	55.7	33	0.506
CJ	18 Jan 2014 11:25	19 Jan 2014 02:10	4.483	2.289	0.017	67.1	29	1.054
BU	21 Jan 2014 10:20	21 Jan 2014 15:50	10.781	2.735	0.034	63.4	21	1.277
BU	21 Jan 2014 18:35	21 Jan 2014 05:50	12.142	2.532	0.038	54.3	28	1.105

Drag Coefficient versus IPS Roughness Scale

There should exist a relationship between the ADCP derived roughness scale, z_o, and the roughness of the ice as observed by the IPS, σ_{IPS}. This relationship does not appear to be linear (Figure 9). However, the drag coefficient derived from z_o at a reference depth of 1 m based on Eq 2, does appear to have a roughly linear relationship with σ_{IPS}. Further refinement of the algorithms to derive z_o and σ_{IPS}, along with finding more events within the extensive ADCP/IPS data sets that are available should improve the fit.

The relationship of drag coefficient to σ_{IPS} ($c_d \sim 0.024 \cdot \sigma_{IPS}$) can be used to estimate turbulence induced drag, at times and locations when there is IPS data but the ADCP is incapable of measuring the logarithmic boundary layer. Standard deviations of the high-passed filtered ice draft were run on 10 km long windows. The windows are approximately the length of ice passing by the ADCPs during the events of Table 1.

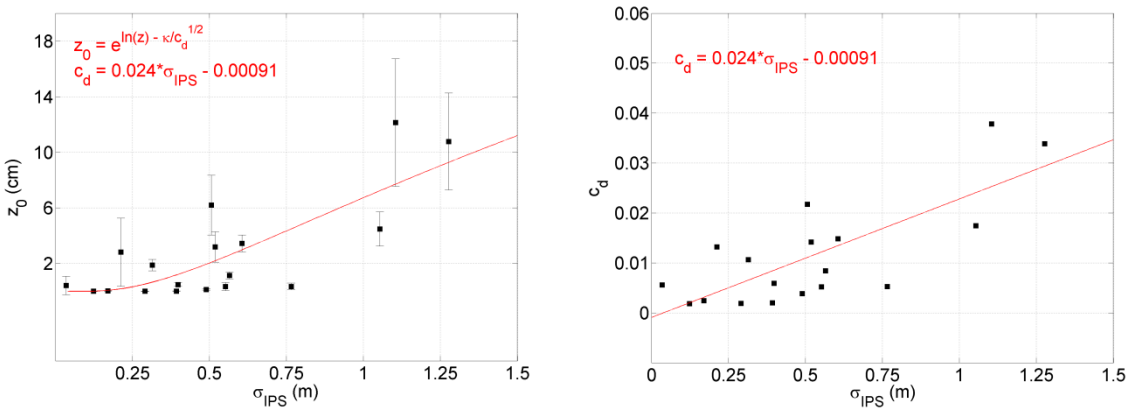

Figure 9. Bottom roughness versus the standard deviation of 300m high pass filtered IPS derived drafts (left). Drag coefficient versus the standard deviation of 300m high pass filtered IPS derived drafts (right).

Drag coefficients derived from the IPS vary both in time and space (Figure 10). Drag coefficients calculated for the early season from November to March, 2012-13, and then the late season from April to July, 2013 at the Crackerjack site show a dramatic change in distribution. The median value more than doubled to over 0.02, late in season as the ice became more deformed. Full ice season distributions of drag coefficients were estimated for three sites: Burger, Camden Bay Site A, and a Department of Fisheries and Oceans Canada site in the Canadian Beaufort. These three regions are of particular interest as we know from Mudge et al (2013), based on multiple site-years of data, the +5 m keel density is greatest at Camden Bay and the least within the Canadian Beaufort. Expectations would be the highest drag coefficients to be in Camden Bay which does not hold for this single ice season.

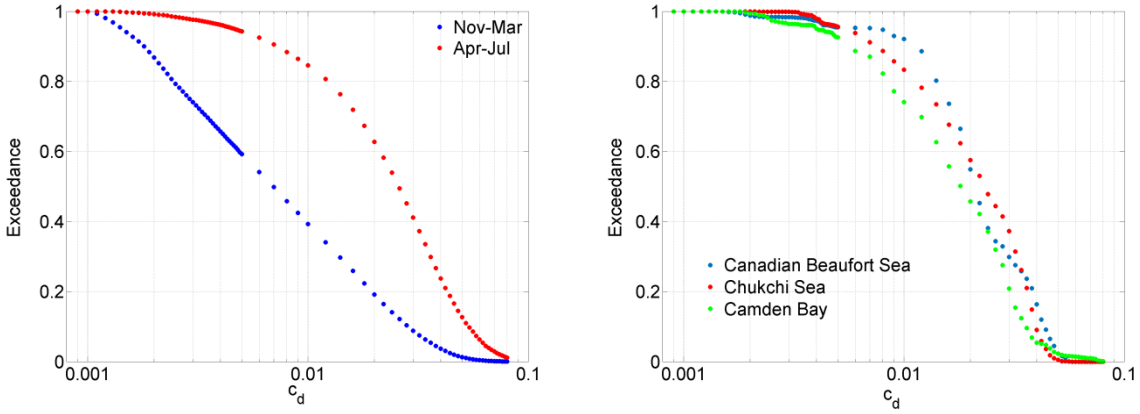

Figure 10. Exceedance of drag coefficient derived from IPS estimated roughness by season at Crackerjack for 2012-13 (left). Exceedance of drag coefficient derived from IPS estimated roughness for Burger Chukchi Sea, Camden Bay Site A, and DFO Site 02 from the Canadian Beaufort Sea (right).

Conclusions

Well developed turbulent logarithmic layers under sea ice are detectable with subsurface ADCPs, during very specific conditions. Eighteen high ice drift speed events in the Chukchi Sea from 2012 to 2014 have provided turbulent parameters, roughness element and friction velocity, under a range of ice canopy conditions – IPS derived sea ice roughness was from 0.04 to 1.3 m. A roughly linear relationship exists between the IPS derived ice roughness and the drag coefficients derived from the turbulent logarithmic layers measured by the ADCPs.

This simple empirical model shows promise in estimating ocean turbulence induced sea-ice drag from any IPS data set. Further work is needed to improve the relationship and confirm that it is not site specific.

Acknowledgements

We would like to thank Olgoonik-Fairweather, prime contractor of the Chukchi Science Environmental Studies program, for their outstanding management and exceptional HSE program and Dr. Humfrey Melling of the Department of Fisheries and Oceans Canada for the use of his ice draft data from the Canadian Beaufort Sea.

REFERENCES

Ekman, V. W., 1905. "On the influence of the earth's rotation on ocean currents". Arch.Math. Astron. Phys., 2, 1{52}.

Fissel, D.B., et al, 2007. "Improvements in upward looking sonar-based sea ice measurements: a case study for 2007 ice features in Northumberland Strait, Canada", in Proceedings of Oceans 2007 Conference, Vancouver, B.C., Canada, 6p. IEEE Press.

Lueck, R. G., and Lu, Y., 1997. "The logarithmic layer in a tidal channel". Cont. Shelf Res. 17, 1785–1801.

McCave I.N., 2005. "Deposition from Suspension", Encyclopedia of Geology: *Sedimentary* Processes, (eds. Selly R.C., Cocks L.R.M., Malone J.M.) Oxford, 5, pp 8-17.

McPhee, M. G. 2013 "The Ice-Ocean Boundary Layer", submitted as a chapter in Sea Ice, Third Edition, edited by David Thomas

Melling, H., Johnston, P.H. and Reidel D.L., 1995. "Measurements of the Underside Topography of Sea Ice by Moored Subsea Sonar*," J. Atmospheric and Ocean Technology*, 12: 589-602.

Mudge, T., Sloat, J. and Chen, J., 2005. "Discharge and Current Profiles Under the Ice", Proceedings of the IEEE/OES Eighth Working Conference on Current Measurement Technology.

Mudge, T., Fissel, D., Milutinovic, M., Borg, K., Sadowy, D. and Ross E., 2013. "Further Improvements to Understandings of Extreme Arctic Sea Ice Thickness Derived From Upward Looking Sonar Ice Data", Proceedings of the POAC'13 Conference, Espoo, Finland, 8p.

Mudge, T., Fissel, D., Milutinovic, M., Borg, K., Sadowy, D. and Ross E., 2014. "The Measurement of Shallow Ocean Currents beneath Deformed Mobile Sea Ice using Upward Looking Sonar Instruments.", Proceedings of the IceTech14 Conference, Banff, AB, Canada, 11p.

Perlin, A., et al, 2005. "A modified law-of-the-wall applied to oceanic bottom boundary layers", J. Geophys. Res., 110, C10S10.

Tennekes, H., and Lumley, J. L., 1972. A first course in turbulence, MIT Press, Cambridge, Mass.